Pure appl. geophys. 159 (2002) 2385–2412
0033–4553/02/102385–28 $ 1.50 + 0.20/0

Pure and Applied Geophysics

Accelerated Seismic Release and Related Aspects of Seismicity Patterns on Earthquake Faults

YEHUDA BEN-ZION[1] and VLADIMIR LYAKHOVSKY[2]

Abstract — Observational studies indicate that large earthquakes are sometimes preceded by phases of accelerated seismic release (ASR) characterized by cumulative Benioff strain following a power law time-to-failure relation with a term $(t_f - t)^m$, where t_f is the failure time of the large event and observed values of m are close to 0.3. We discuss properties of ASR and related aspects of seismicity patterns associated with several theoretical frameworks. The subcritical crack growth approach developed to describe deformation on a crack prior to the occurrence of dynamic rupture predicts great variability and low asymptotic values of the exponent m that are not compatible with observed ASR phases. Statistical physics studies assuming that system-size failures in a deforming region correspond to critical phase transitions predict establishment of long-range correlations of dynamic variables and power-law statistics before large events. Using stress and earthquake histories simulated by the model of BEN-ZION (1996) for a discrete fault with quenched heterogeneities in a 3-D elastic half space, we show that large model earthquakes are associated with nonrepeating cyclical establishment and destruction of long-range stress correlations, accompanied by nonstationary cumulative Benioff strain release. We then analyze results associated with a regional lithospheric model consisting of a seismogenic upper crust governed by the damage rheology of LYAKHOVSKY *et al.* (1997) over a viscoelastic substrate. We demonstrate analytically for a simplified 1-D case that the employed damage rheology leads to a singular power-law equation for strain proportional to $(t_f - t)^{-1/3}$, and a nonsingular power-law relation for cumulative Benioff strain proportional to $(t_f - t)^{1/3}$. A simple approximate generalization of the latter for regional cumulative Benioff strain is obtained by adding to the result a linear function of time representing a stationary background release. To go beyond the analytical expectations, we examine results generated by various realizations of the regional lithospheric model producing seismicity following the characteristic frequency-size statistics, Gutenberg-Richter power-law distribution, and mode switching activity. We find that phases of ASR exist only when the seismicity preceding a given large event has broad frequency-size statistics. In such cases the simulated ASR phases can be fitted well by the singular analytical relation with $m = -1/3$, the nonsingular equation with $m = 0.2$, and the generalized version of the latter including a linear term with $m = 1/3$. The obtained good fits with all three relations highlight the difficulty of deriving reliable information on functional forms and parameter values from such data sets. The activation process in the simulated ASR phases is found to be accommodated both by increasing rates of moderate events and increasing average event size, with the former starting a few years earlier than the latter. The lack of ASR in portions of the seismicity not having broad frequency-size statistics may explain why some large earthquakes are preceded by ASR and other are not. The results suggest that observations of moderate and large events contain two complementary end-member predictive signals on the time of future large earthquakes. In portions of seismicity following the characteristic earthquake distribution, such information exists directly in the associated quasi-periodic temporal distribution of large events. In portions of seismicity having broad frequency-size statistics with

[1] Department of Earth Sciences, Univ. of Southern CA, Los Angeles, CA, 90089-0740, U.S.A. E-mail: benzion@terra.usc.edu

[2] Geological Survey of Israel, 30 Malkhei Israel, Jerusalem 95501, Israel. E-mail: vladi@geos.gsi.gov.il

random or clustered temporal distribution of large events, the ASR phases have predictive information. The extent to which natural seismicity may be understood in terms of these end-member cases remains to be clarified. Continuing studies of evolving stress and other dynamic variables in model calculations combined with advanced analyses of simulated and observed seismicity patterns may lead to improvements in existing forecasting strategies.

Key words: Continuum mechanics, damage rheology, heterogeneous faults, seismicity patterns, large earthquake cycles.

1. Introduction

Large earthquakes are often, but not always, preceded by a period during which the surrounding region experiences a phase of accelerated seismic release (ASR). This may be manifested as higher overall seismicity rates or elevated rates of low magnitude seismicity (e.g., PAPAZACHOS, 1973; JONES and MOLNAR, 1979; SHAW *et al.*, 1992), increasing earthquake magnitude and/or number of moderate-size events with time (e.g., MOGI, 1969, 1981; ELLSWORTH *et al.*, 1981; LINDH, 1990; KNOPOFF *et al.*, 1996), and/or higher values of several functions of those (e.g., VARNES, 1989; SYKES and JAUMÉ, 1990; KEILIS-BOROK and KOSSOBOKOV, 1990; BUFE and VARNES, 1993; PRESS and ALLEN, 1995). The various forms of ASR activities occur in a broad region surrounding the following large earthquake ruptures. A recent review of features associated with observed ASR phases can be found in JAUMÉ and SYKES (1999).

BUFE and VARNES (1993) analyzed a few cumulative measures of seismic release during a period of about 150 years in northern California in terms of a power-law time-to-failure relation

$$\sum \mathrm{M}_0^{\zeta}(t) = \mathrm{A} + \mathrm{B}(t_{\mathrm{f}} - t)^m \ , \tag{1a}$$

where t is time, A, B, and m are adjustable parameters, t_{f} is failure time of a relatively large earthquake terminating a phase of ASR, and M_0^{ζ} is seismic moment for $\zeta = 1$, event count for $\zeta = 0$, and Benioff strain for $\zeta = 1/2$. They concluded that the cumulative Benioff strain in the space-time domain they study follows the power-law relation (1a) better than either a cumulative event count or cumulative seismic moment. SYKES and JAUMÉ (1990) fitted cumulative moment release in a similar space-time domain to that used by BUFE and VARNES (1993) with an exponential, rather than a power law function.

Subsequent observational analyses of ASR before relatively large earthquakes (BUFE *et al.*, 1994; SORNETTE and SAMMIS, 1995; VARNES and BUFE, 1996; BOWMAN *et al.*, 1998; BREHM and BRAILE, 1998; ROBINSON, 2000) focused on power-law time-to-failure fits of cumulative Benioff strain

$$\sum \mathrm{M}_0^{1/2}(t) = \mathrm{A} + \mathrm{B}(t_{\mathrm{f}} - t)^m \ . \tag{1b}$$

In retrospective- and forward-prediction applications of (1b) (e.g., BUFE *et al.*, 1994; SORNETTE and SAMMIS, 1995; BREHM and BRAILE, 1999; ROBINSON, 2000), values of t_f and A found by fitting procedures give estimates of the time and magnitude of the events culminating the ASR phases. It is well known (e.g., KANAMORI and ANDERSON, 1975) that event count N, earthquake magnitude M, and seismic moment M_0 of regional seismicity satisfy the scaling relations $\mathrm{Log}_{10}N \sim -M$ and $\mathrm{Log}_{10}M_0 \sim 1.5$ M. Thus applications of (1a) with $\zeta = 1$ and $\zeta = 0$ give dominating weights to the largest and smallest events within the analysis, respectively, while fractional values of ζ provide filters that modify the relative contributions of events in different magnitude ranges. With the above scaling relations, the contribution from each magnitude unit is approximately the same for $\zeta = 2/3$, and consequently the choice $\zeta = 1/2$ in (1b) associated with the Benioff strain gives a somewhat higher weight to smaller events (e.g., SAMMIS *et al.*, 1996).

Table 1 summarizes information on seismic regions, culminating large earthquakes, and best-fitting or fixed-used values of the exponent m in observational studies of ASR employing Benioff strain. We note that the number N of data points used to estimate the parameters of (1b) from observed ASR phases is typically less than 30. Synthetic data tests indicate that the uncertainty of estimated power-law parameters, approximately proportional to $N^{1/2}$, is rather high for such small data sets (Y. Huang, pers. comm., 2000). In addition, there are other possible errors in the best-fitting and used m values (and other ASR parameters) due to ambiguities associated with the identification of ASR phases, selection of involved spatio-temporal domains, and various other analysis issues (e.g., VERE-JONES *et al.*, 2001). Nevertheless, the results summarized in Table 1 form the current phenomenological basis of ASR and as such they are used in the present work. The relatively large earthquakes terminating the observed ASR phases range in size from $M < 4$ (BREHM and BRAILE, 1998) to $M > 8$ (BUFE *et al.*, 1994; BOWMAN *et al.*, 1998). Figures 1a and 1b show the distributions of all and best-fitting m values of Table 1, calculated with the kernel density method (SILVERMAN, 1986). The two distributions are peaked at m values of 0.29 and 0.28, respectively. Figures 1c and 1d show the mean, standard deviation, and median of all and best-fitting m values as a function of the magnitude cutoff M_{cut} of the relatively large events terminating the observed ASR phases. In both Figures 1c and 1d, the mean and median have a flat maximum region near $m = 0.3$ for $5 \leq M_{cut} \leq 7.5$ and they fall for smaller and larger M_{cut}.

In the following sections we present analytical and numerical results on ASR phases and related properties of seismicity patterns based on a number of different theoretical models. In Section 2.1 we discuss expectations associated with subcritical crack growth and conclude that this framework provides an inadequate explanation for observed ASR phases. In Section 2.2 we review statistical physics studies based on the assumption that large events in a deforming region correspond to phase transitions. Generic expectations in this framework include progressive establishment of long-range correlations of dynamic variables and

Table 1

Reported best-fitting and fixed-used values of the exponent m of the power-law time-to-failure equation (1b) in observational studies of accelerated seismic release

References	Seismic region	M large	m_{free}	m_{used}	Notes
Bufe and Varnes [1993] (BV 93)	Branches of the San Andreas fault system north of the creeping zone	7.9 6.9 6.8	0.32 0.30 0.34		
Bufe et al. [1994] (BNV 94)	Segments of subduction zone in the Alaska-Aleutian region	7.5 7.4 7.8 7.8 8.5		0.3 0.3 0.3 0.3 0.3	
Sornette and Sammis [1995] (SS95)	Loma Prieta Kommandorski Island	6.9 >8.0	0.35, 0.34* 0.26, 0.28*		* denotes values obtained using equation (6), where the power law (1b) is augmented by log-periodic oscillations. Same sequences were also studied by BV93 and BNV94
Varnes and Bufe [1996] (VB96)	Virgin Islands	4.8 4.8		0.2 0.3	
Bowman et al. [1998]	California	7.5 7.3 7.0 6.7 6.7 6.6 6.6 6.5 7.7 5.6	0.3 0.18 0.28 0.18 0.1 0.13 0.43 0.55 0.49 0.12		Some sequences also studied by BV93, SS95, and VB96
	Assam Virgin Islands	8.6 4.8	0.22 0.11		
Brehm and Brail [1998]	New Madrid seismic zone	6.2 5.5 4.3 3.6 3.8 4.3 3.6 3.5 3.6 5.2 4.1 4.3 3.8	0.13 0.27 0.25 0.27 0.20 0.27 0.13 0.30 0.35 0.16 0.23 0.12 0.30		

Table 1

Continued

References	Seismic region	M large	m_{free}	m_{used}	Notes
Brehm and Brail [1998]	New Madrid seismic zone	4.3	0.20		
		4.8	0.16		
		3.9	0.27		
		3.5	0.18		
		4.2	0.24		
		3.5	0.47		
Robinson [2000]	New Zealand	7.0	0.31		
		6.7	0.29		
		6.7	0.46		

asymptotic power-law relations during the evolution leading to critical or spinodal phase transitions (e.g., SORNETTE and SAMMIS, 1995; SALEUR *et al.*, 1996; RUNDLE *et al.*, 2000b). In Section 2.3 we show that large earthquakes in the model of BEN-ZION (1996) for a discrete heterogeneous strike-slip fault in a 3-D elastic half space are associated with non-repeating cyclical establishment and destruction of long-range stress correlations accompanied by non-stationary cumulative Benioff strain. In Section 2.4 we demonstrate analytically that a 1-D version of the damage rheology of LYAKHOVSKY *et al.* (1997) leads to a power-law time-to-failure relation for strain with $m = -1/3$, and a corresponding power law for cumulative Benioff strain with $m = 1/3$. To derive an approximate expectation for regional deformation we add to the latter result a linear function of time representing release from background seismicity. Properties of evolving seismicity patterns in a regional model consisting of a seismogenic upper crust governed by the damage rheology of LYAKHOVSKY *et al.* (1997) over a viscoelastic substrate are discussed in Section 2.5. The results indicate that power-law build-up of cumulative Benioff strain exists only when the seismicity preceding the large earthquakes has broad frequency-size (FS) statistics. In such cases, the simulated ASR phases can be fitted well by all three forgoing analytical results. The ASR phases in the model simulations are accommodated both by increasing average rate of moderate events and increasing average earthquake size, with the former beginning a few years earlier. A brief discussion of the results including suggestions for future studies and implications for forecasting large event times is given in Section 3.

2. Analysis

Several theoretical frameworks may be used to explain the origin and parameters of the time-to-failure power-law relation of cumulative Benioff strain. These include

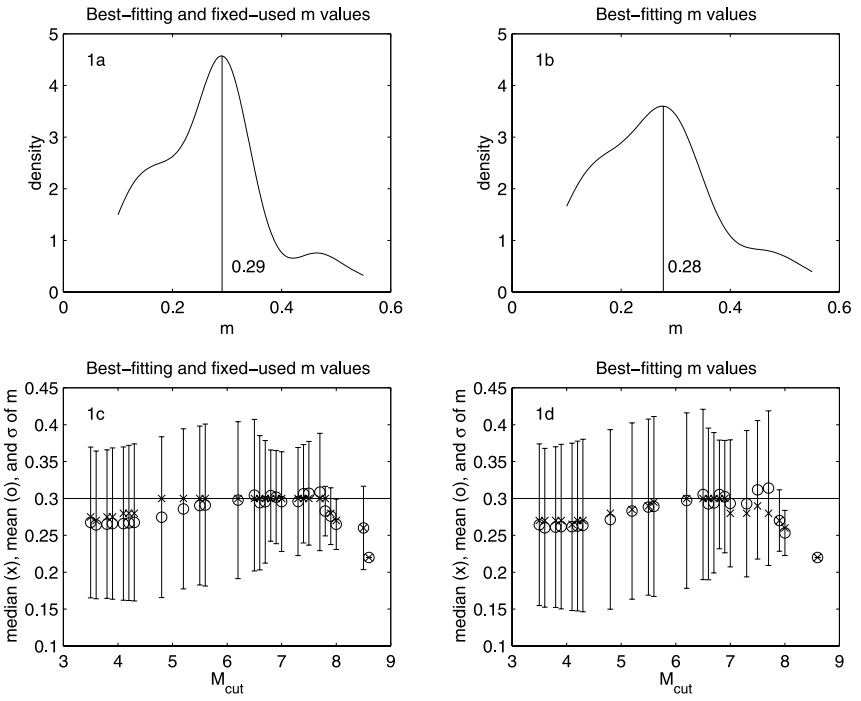

Figure 1
Statistics of best-fitting and fixed-used *m* values in the observations summarized in Table 1. (a) Density (smooth histogram) of all the *m* values of Table 1 calculated with the kernel density method. (b) Same as (a) for the best-fitting values only. (c) Median (x), mean (o), and standard deviation (vertical error bars) for all *m* values of Table 1 as a function of magnitude cutoff of the events terminating the reported accelerated seismic release (ASR) phases. (d) Same as (c) for the best-fitting *m* values only.

sub-critical crack growth, phase transition, and brittle deformation of heterogeneous faults in continuum solids. The first approach provides a deterministic description of failure at a single (relatively small, microscopic or mesoscopic) scale based on continuum mechanics. The second gives macroscopic statistical physics results for multi-scale failures near conditions of a global phase transition. The third, which we develop further in this work, incorporates elements of the other two.

2.1. Subcritical Crack Growth

In solids with microcracks, inclusions, and other flaws, the internal stress field is highly non-uniform. Such materials subjected to long-term loading show significant rates of macroscopic crack extension at nominal (macroscopic) values of stress intensity factor K significantly lower than the critical value for brittle failure. This phenomenon is known as subcritical crack growth (SWANSON, 1984; ATKINSON and MEREDITH, 1987; INGRAFFEA, 1987; COX and SCHOLZ, 1988). Experimental rates of

subcritical crack growth are most commonly represented by a power-law equation (CHARLES, 1958; PARIS and ERDÖGAN, 1963)

$$\frac{dL}{dt} = C \cdot K^p \quad , \tag{2}$$

where L is crack length and C and p are material parameters depending on confining pressure, temperature, and other conditions. The latter is referred to as crack index or stress corrosion index. Observed values of p in laboratory experiments vary greatly during crack evolution (SWANSON, 1984, 1987; MEREDITH and ATKINSON, 1985; ATKINSON and MEREDITH, 1987). In slow early deformation phases, p typically ranges from 2 to 5. Then p may decrease slightly in a regime apparently controlled by transport rates of reactive species at the crack tip. At some critical crack length there is a transition to dynamic rupture and p increases rapidly to values between 10 and 100. LYAKHOVSKY (2001) demonstrates that calculated rates of quasi-static crack propagation in a solid governed by the damage rheology of LYAKHOVSKY *et al.* (1997) fit the above observations of subcritical crack growth.

DAS and SCHOLZ (1981), VARNES (1989), BUFE and VARNES (1993), MAIN (1999) and others use the square-root relation between crack intensity factor and crack length to convert (2) into a differential equation for crack growth in the form

$$\frac{dL}{dt} = C^* L^{p/2} \quad , \tag{3}$$

where C^* depends on the applied load (assumed constant), pressure, temperature and material properties. Integrating (3) and writing the solution for a crack growing from an initial length L_0 gives

$$L = [L_0^{(2-p)/2} - (p-2)C^* t/2]^{2/(2-p)} \quad . \tag{4}$$

For $p > 2$, the crack length diverges when the quantity in the bracket becomes zero. Using this to define a failure time (e.g., DAS and SCHOLZ, 1981) and substituting back to (4) and (3) lead to a power-law relation between the crack length and time-to-failure. To connect the result with (1a) and (1b), we use a scaling relation $M_0 \sim L^\eta$ between seismic moment and crack dimension. The values of the exponent η range from 3 for a smooth classical crack (e.g., KANAMORI and ANDERSON, 1975) to 2 for a disordered fractal-like rupture (FISHER *et al.*, 1997). Accounting for the square-root conversion from seismic moment to Benioff strain, the relation between the exponent m in (1b) and crack index p is

$$m = \eta/(p-2) \quad . \tag{5}$$

Using (5) and observed values of p, we estimate the values of m expected to be associated with different stages of the subcritical crack growth process. During the initial slow stage of crack growth ($p = 2 - 5$), m varies from an unbounded value to 1

or 2/3 depending on whether η is 3 or 2. This regime probably represents very low seismic activity below the levels associated with observed ASR phases. During the transitional regime before dynamic rupture, p increases, m decreases, and both vary greatly. For $p > 32$ (or 22), m drops below 0.1 for $\eta = 3$ (or 2). The predicted high variability of m in the transition to dynamic rupture and low asymptotic value before large-scale failure are not compatible with the values of m estimated from observed ASR phases (Table 1 and Fig. 1).

The framework of subcritical crack growth was developed originally as an empirical description of laboratory observations involving primarily the evolution of a single crack from an early quasi-static deformation at small size scales to an unstable dynamic rupture at a critical length. This may be referred to as a deterministic continuum mechanics approach at a relatively small single scale. In contrast, the ASR phenomenology is associated with a network of faults at a variety of scales in a broad region around the eventual rupture that terminates an ASR phase. It thus appears that subcritical crack growth before a large dynamic failure on a fault does not provide a satisfactory explanation of ASR, both conceptually and in terms of stability and asymptotic value of the m exponent.

2.2. Phase Transition

An alternative approach to understanding ASR based on statistical physics of critical phenomena was developed by SORNETTE and SAMMIS (1995), SAMMIS *et al.* (1996), and SALEUR *et al.* (1996). The basic underlying assumption in this approach is that large earthquakes represent phase transitions in some extended spatial domain where stress is correlated and close to a critical level for a system-size failure. With additional assumptions and appropriate theoretical developments, this framework provides (in contrast to the subcritical crack approach) asymptotic statistical results for multi-scale failures in the space-time regions near the largest failure event. In this view, phases of ASR are associated with a progressive occurrence of increasingly larger events, due to progressive establishment of stress correlations over larger portions of a given seismogenic domain. The latter may be defined as a region where stress interaction with the tectonic loading and seismicity patterns are dominated by large earthquakes on a major through-going fault zone.

BEN-ZION and SAMMIS (2001) review a variety of observational and theoretical works on the character of fault zones and suggest that large-scale tectonic deformation in given crustal domains is indeed dominated by relatively regular, major through-going fault zones. This situation holds in the model of BEN-ZION (1996) for a single disordered strike-slip fault system in a 3D elastic half space discussed in Section 2.3, and the regional lithospheric model of BEN-ZION *et al.* (1999) and LYAKHOVSKY *et al.* (2001) discussed in Section 2.5. In practice, however, it is not yet clear how to divide the seismogenic crust into dominating fault zones and associated surrounding domains in the sense discussed above. BOWMAN *et al.* (1998),

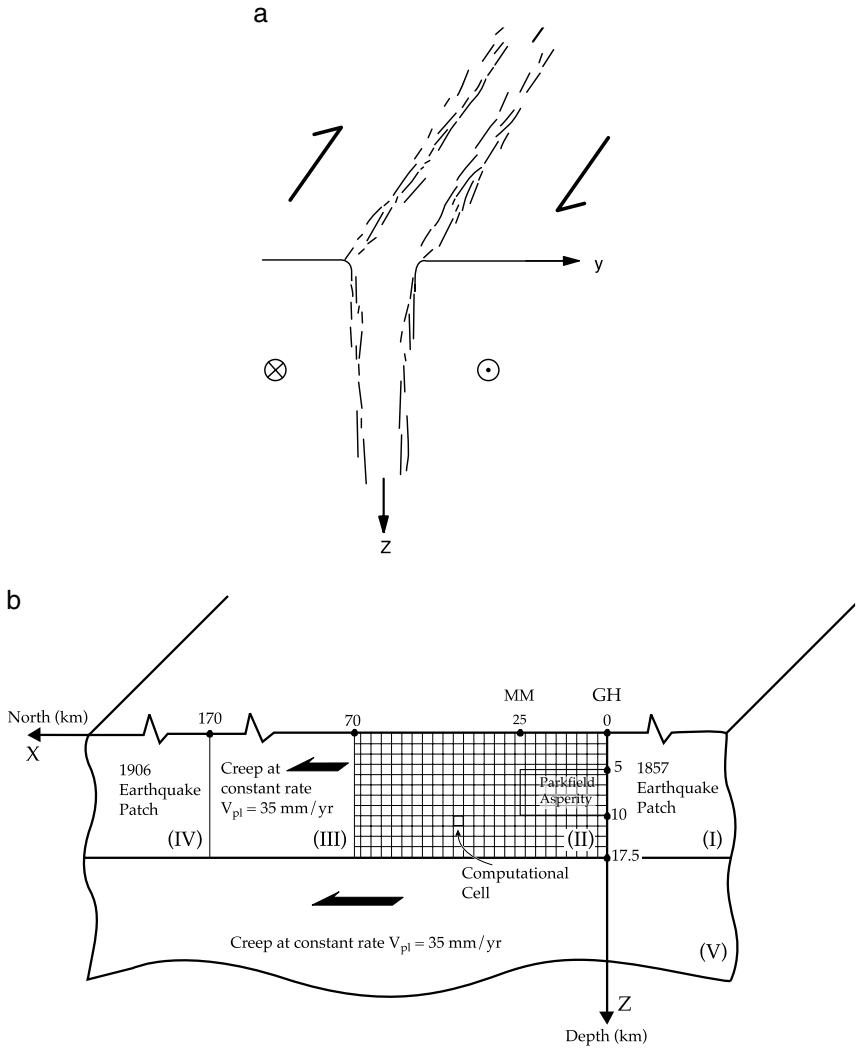

Figure 2

(a) A schematic representation of a 3-D disordered strike-slip fault structure (from BEN-ZION, 1996). (b) A planar representation of a disordered fault zone by a 2-D heterogeneous fault embedded in a 3-D elastic half-space. Each fault location $(x, y = 0, z)$ represents deformation in a volume centered on the line (x, y, z). The geometric disorder is modeled as disorder in strength properties of the planar fault. On regions I, II, IV, V, boundary conditions are specified. Region II is a computational grid where spatio-temporal evolution of stress and slip are calculated. The shown model configuration is tailored for the central San Andreas Fault. GH and MM mark approximate positions of Gold Hill and Middle Mountain (from BEN-ZION, 1996).

BREHM and BRAILE (1998), and ROBINSON (2000) identified about 30 crustal domains that were associated with phases of ASR before past large earthquakes, using search procedures that maximize the fit between observed cumulative Benioff strain and the

time-to-failure power-law relation (1b). ZOLLER *et al.* (2001) identified about ten such domains (most of which overlap with and are somewhat larger than those of BOWMAN *et al.* (1998)) by optimizing the fit between growing correlations of hypocenter locations and power-law time-to-failure relation. It is important to examine in future works whether the regions defined in those studies based on past seismicity will preserve their intended functionality in the context of new ASR phases.

SORNETTE and SAMMIS (1995), SAMMIS *et al.* (1996), and SALEUR *et al.* (1996) applied the renormalization group theory to show that cumulative Benioff strain may represent the scaling regime of a critical phase transition, and that a complex-valued critical exponent produces log periodic correction to the right side of (1b),

$$\sum \mathrm{M}_0^{1/2}(t) = \mathrm{A} + \mathrm{B}(t_\mathrm{f} - t)^m [1 + \mathrm{C}\cos(2\pi \log(t_\mathrm{f} - t)/\log(\lambda) + \psi)] \ , \qquad (6)$$

with C, λ, and ψ being three additional free parameters. They also showed (SALEUR *et al.*, 1996) that complex critical exponents might be generated by an underlying structure with discrete scale invariance (i.e., scale invariance at specific discrete magnifications) or a Euclidean heterogeneous system in which discrete scale invariance is produced by the dynamics. HUANG *et al.* (2000) demonstrated that log periodic oscillations in cumulative Benioff strain are also the expected generic outcome of routine processing of data containing an underlying power-law structure as in (1a) and (1b) with superimposed white noise. The integration to obtain cumulative Benioff strain transforms the original white noise to a correlated signal that is manifested as log periodic oscillations around the background power-law buildup. SORNETTE (1992) found that the mean field value of the exponent m associated with a critical phase transition is $m = 1/2$. This is close to the upper range rather than the mean or median of the observed m values with a peak around 0.3 (Table 1 and Fig. 1). RUNDLE *et al.* (2000b) used scaling arguments to show that power-law time-to-failure buildup of cumulative Benioff strain may represent the scaling regime of a spinodal phase transition, with an exponent $m = 1/4$ close to the observed values.

The statistical physics analyses provide powerful tools for studying possible types and statistical properties of event patterns. However, they cannot be used to calculate details of stress and displacement fields in a deforming solid. In the following sections we discuss results based on deterministic models of heterogeneous faults with many degrees of freedom in continuum solids. These heterogeneous models account for both complex evolving seismicity patterns with multi-scale failures and detailed deformation fields of the associated individual events.

2.3. Seismicity Patterns on Discrete Fault Systems with Quenched Heterogeneities

BEN-ZION (1996) simulated seismicity patterns for various cases of a 2-D discrete fault system in a 3-D elastic solid, based on earlier works of BEN-ZION and RICE

(1993, 1995). The model incorporates long-range elasticity, classical static/kinetic friction, power law creep, realistic boundary conditions, and various types of quenched heterogeneities. The work attempts to clarify the seismic response, on time scales of a few hundreds of years, of large individual fault systems, which have various levels of geometric disorder in the spatial distribution of brittle properties. A basic assumption of the model is that over such time scales the first-order deformational processes in a long and narrow 3-D fault zone (Fig. 2a) can be mapped onto a 2-D planar fault in a 3-D elastic solid (Fig. 2b). As discussed in Section 2.5, this is supported by good overall agreement between seismicity patterns generated by various cases of quenched heterogeneities in the planar model, and corresponding cases in the regional lithospheric model of LYAKHOVSKY *et al.* (2001) and BEN-ZION *et al.* (1999) with evolving non-planar structures. However, a rigorous mapping of various forms of 3-D geometric disorder onto corresponding planar representations remains an important unresolved issue.

The results of BEN-ZION (1996, Figs. 8–11) show that during gradual tectonic loading, small and intermediate earthquakes produce stress-roughening over their size scales, which collectively smooth the longer wavelength components of stress and develop long-range stress correlations on the fault. The pattern is reversed during large ruptures of size approaching the system dimension, which reduce the stress level and smooth the fluctuations along the large rupture area, while creating large stress concentrations near its boundary and increasing considerably the stress outside it. These system-size events reroughen the long wavelength stress field on the fault, destroy the long-range correlation in the system, and set the beginning of a new large earthquake cycle. ENEVA and BEN-ZION (1999) analyzed the progressive establishment and destruction of stress correlations in the simulated results using fluctuations of a stress-based order parameter. Following FERGUSON (1997) who evaluated slip-deficit fluctuations in a slider-block model, the analysis employs a stress fluctuation variable $F(t)$ defined as

$$F(t) = \sqrt{\frac{1}{K}\sum_{i=1}^{K}(\tau_i(t) - \bar{\tau}_i)^2} \ , \tag{7}$$

where $\tau_i(t)$ is the stress at cell i and time t, $\bar{\tau}_i$ is the temporal average of stress at cell i during the deformation history, and K is the total number of computational cells. The variable $F(t)$ gives the temporal evolution of the RMS stress fluctuations along the fault. Increasing fluctuations correspond to increasing spatial correlation and increasing proximity to a global critical state.

Figure 3 top gives $F(t)$ of (7) for 150 years of deformation history simulated by the model realization of BEN-ZION (1996) with a fractal distribution of strength heterogeneities. The results show clearly the existence of non-repeating cyclic establishment and destruction of stress correlations on the fault. A large cycle begins when each large event (vertical lines in Fig. 3 top) destroys the long-range correlation

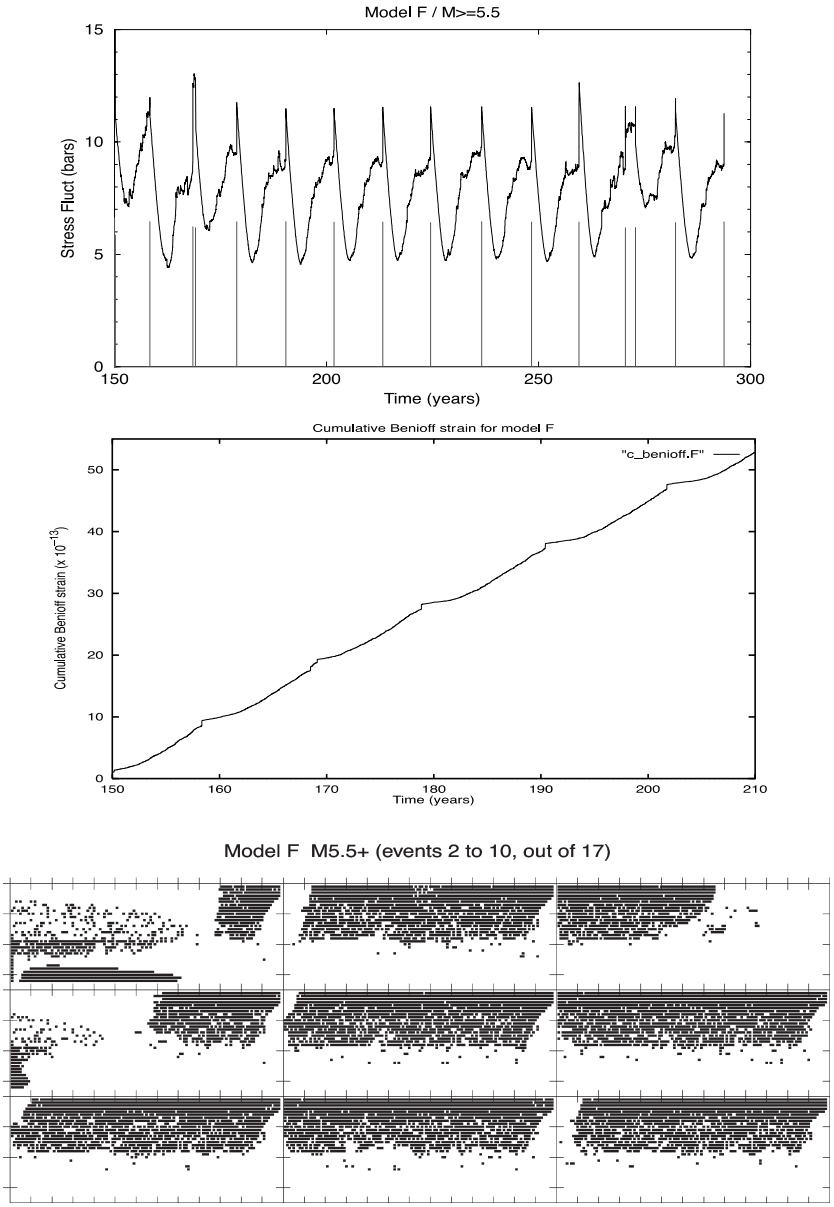

Figure 3

Top panel: Fluctuations of a stress-based order parameter for the model realization of BEN-ZION (1996) with fractal distribution of strength heterogeneities. The vertical lines show the times of 17 events with $M \geq 5.5$ that occur in the calculated history. Middle panel: Cumulative Benioff strain in the first 60 years of model evolution with 5 large earthquake cycles. Bottom panel: Rupture areas of events 2–10 of the 17 $M \geq 5.5$ earthquakes shown in the top panel. The event number increases from left to right and top to bottom (i.e., event 2 is on the left of the top raw and event 10 is on the right of the bottom raw).

of stress fluctuations. The combined occurrences of the subsequent small to intermediate size events increase the spatial correlation of fluctuations on the fault. The correlation length reaches a maximum value at about 3/4 the cycle time, when the ongoing model events establish "stress bridges" across the entire system. Then the correlation length fluctuates around the maximum value, sometimes with one or more clear drops, until one small event cascades to become the next large earthquake. This destroys the long-range correlation and starts a new cycle. The middle panel in Figure 3 shows the cumulative Benioff strain release on the fault for the first 60 years with five large earthquake cycles. As seen, there is clear overall correspondence between the cumulative Benioff strain, increasing stress correlation, and large earthquake cycle on the fault. However, since the model of Figure 2 does not simulate regional seismicity, the nonlinearities in the cumulative Benioff strain are produced primarily by drops after rather than build up before large events. Figure 3 bottom shows rupture areas of 9 large events that set the cycles duration. The areas are not necessarily contiguous, since the model incorporates long-range elasticity, however all these ruptures produce system-size stress changes that punctuate the relatively gradual preceding and following evolving correlations.

The simulated establishment and destruction of stress correlations within large earthquake cycles represent a nonrepeating cyclical approach to and retreat from criticality, or intermittent criticality, in general agreement with the cellular automata simulations of SAMMIS and SMITH (1999). Intermittent criticality associated with the occurrence of large earthquakes is supported by observed power law distributions of moment vs. time (ASR phases), number vs. moment (Gutenberg-Richter frequency-size statistics), and number vs. time (Omori law) before and after large earthquakes. We note that FISHER *et al.* (1997) demonstrated analytically and numerically that the model of BEN-ZION (1996) has an underlying critical point of a second-order phase transition. The critical point is associated with specific values of tuning parameters (dynamic weakening and conservation of stress transfer during failure events), and therefore it is "standard-ordinary-criticality" rather than "self-organized-criticality." In addition, the dynamics of the fault system of Figure 2 have a clear cyclical component, whereas self-organized-criticality describes stationary criticality where the only deviations from power-law distributions are statistical fluctuations (e.g., JENSEN, 1998). Tuning parameters and cyclical components are also present in the dynamics of the regional model for coupled evolution of earthquakes and faults discussed in the following two sections.

2.4. Continuum-mechanics-based Damage Rheology Model

BEN-ZION *et al.* (1999) and LYAKHOVSKY *et al.* (2001) used the damage rheology model of LYAKHOVSKY *et al.* (1997) in a regional lithospheric framework employed in the next section. The damage rheology of LYAKHOVSKY *et al.* (1997) provides a continuum-mechanics-based formulation for evolving non-linear properties of rocks

under conditions of irreversible deformation. The framework adds to the Lamé parameters of linear Hookean elasticity λ and μ, a third parameter γ to account for the asymmetry of rock deformation under compression and tension conditions, and makes the moduli functions of an evolving damage state variable α. The damage variable α represents the local microcrack density as a function of the deformation history. An undamaged solid with $\alpha = 0$ is the ideal linear elastic material governed by the usual Hooke's law ($\gamma = 0$ for $\alpha = 0$). At the other extreme, a material with $\alpha = \alpha_c \leq 1$ is densely cracked and can not support any load. The damage rheology model of LYAKHOVSKY *et al.* (1997) calculates the instantaneous values of the elastic moduli for all intermediate states of the damage parameter ($0 < \alpha < \alpha_c$), based on the balance equations of energy and entropy and the above generalization of linear elasticity.

A full derivation of the governing equations and comparisons of model predictions with friction, fracture, and acoustic emission rock mechanics experiments (used both to validate the formulation and to constrain model parameters) are given by LYAKHOVSKY *et al.* (1997). The final equation for damage evolution, used below to derive a power-law time-to-failure relation, is

$$d\alpha/dt = CI_2(\xi - \xi_0) \ , \tag{8}$$

where $\xi = I_1/\sqrt{I_2}$, $I_1 = \varepsilon_{kk}$ and $I_2 = \varepsilon_{ij}\varepsilon_{ij}$ are the first and second invariants of the strain tensor ε_{ij}, the coefficient C describes the rate of damage evolution for a given deformation, and the critical strain parameter ξ_0 is qualitatively similar to internal friction in Mohr-Coulomb yielding criteria. A state of strain $\xi > \xi_0$ leads to material degradation (weakening of instantaneous elastic moduli) with a rate proportional to the second strain invariant multiplied by $(\xi - \xi_0)$. Similarly, a state of strain $\xi < \xi_0$ results in material strengthening (healing of instantaneous elastic moduli) proportional to the same factors. The damage rate coefficient C is constant during material degradation ($\xi > \xi_0$) and an exponential function of α during healing ($\xi < \xi_0$). The latter produces logarithmic healing in agreement with laboratory rate and state friction experiments (e.g., DIETERICH, 1972; SCHOLZ, 1990; MARONE, 1998).

BUFE and VARNES (1993) discuss general connections between ASR and damage mechanics. Below we show that a 1-D version of the damage rheology of LYAKHOVSKY *et al.* (1997) leads with a straightforward analytical derivation to power-law time-to-failure relation for strain with exponent $m = -1/3$, and corresponding power-law relation for cumulative Benioff strain release with $m = 1/3$. For 1-D deformation, equation (8) becomes

$$d\alpha/dt = C\varepsilon^2 \ , \tag{9}$$

where ε is the current strain. The stress-strain relation in this case is

$$\sigma = \mathrm{E}_0(1 - \alpha)\varepsilon \ , \tag{10}$$

where $E_0(1-\alpha)$ is the effective elastic modulus of a 1-D damaged material with E_0 being the initial modulus of the undamaged solid. Assuming constant stress σ and integrating (9) using (10) gives

$$\alpha = 1 - \{1 - (3C\sigma^2/E_0^2)t\}^{1/3} \quad . \tag{11}$$

Substituting (11) back into (10) leads to strain accumulation in the power-law form

$$\varepsilon = \sigma/E_0\{1 - (3C\sigma^2/E_0^2)t\}^{-1/3} \quad . \tag{12}$$

Using in (12) $t_f = E_0^2/3C\sigma^2$, defined by setting $\alpha = 1$ in (11), and changing constants gives

$$\varepsilon(t) = \sigma/E_0(1 - t/t_f)^{-1/3} = \sigma/E_0(\Delta t/t_f)^{-1/3} \tag{13}$$

with $\Delta t = t_f - t$. Equation (13) with negative exponent and strain singularity at the final failure time provides an appropriate physical expression for analyzing evolving deformation preceding a system-size event. However, analysis of observed ASR phases to date have focused on a nonsingular power-law time-to-failure equation of cumulative Benioff strain release with a positive exponent. Such an expression can be readily derived from the previous results. Using (10)–(13), the strain energy is

$$U(t) = (1/2)\sigma\varepsilon = (\sigma^2/2E_0)(\Delta t/t_f)^{-1/3} \quad , \tag{14}$$

the energy and moment releases are proportional to

$$-\partial U/\partial t \sim -(\Delta t/t_f)^{-4/3} \quad , \tag{15}$$

and the cumulative Benioff strain release is proportional to

$$-\int (\partial U/\partial t)^{1/2} dt \sim (\Delta t/t_f)^{1/3} \quad . \tag{16}$$

Thus the 1-D version of our damage rheology predicts a power-law time-to-failure relation for cumulative Benioff strain with an exponent $m = 1/3$, close to the observed values.

Application of equation (16) to data of regional deformation containing many "damage degrees of freedom" requires modifications. The simplest generalization of the above result for such cases may be obtained by adding to the right side of (16) a linear function representing a stationary release associated with background regional seismicity (see also MAIN (1999)). With this, the expected cumulative Benioff strain in regional deformation has the form

$$\sum M_0^{1/2}(t) = A_1 + A_2 t + A_3(\Delta t/t_f)^{1/3} \quad , \tag{17}$$

where A_1, A_2, A_3 are constants. In the next section we use equations (13), (16), and (17) to fit phases of ASR simulated by a regional lithospheric model with a

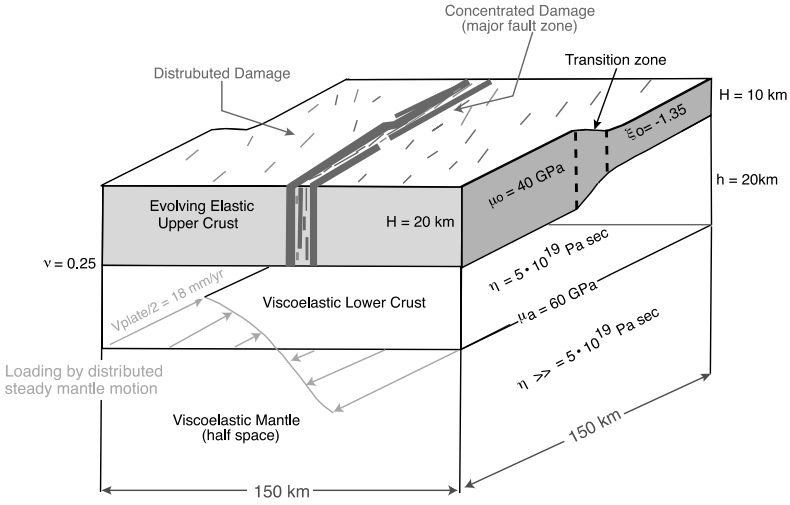

Figure 4

Geometry and parameters for a regional lithospheric model for coupled evolution of earthquakes and faults. The crust consists of a brittle upper layer governed by damage rheology over a viscoelastic lower crust driven by steady mantle motion from below. H and h mark the thickness of the upper and lower crust layers, respectively. Parameters μ, ξ, η, and v denote rigidity, critical strain coefficient, viscosity, and Poisson's constant, respectively. The boundary conditions are constant stress at the left and right edges and periodic repeats at the front and rear faces. The simulations leading to Figures 5 and 6 are done with a uniform crustal thickness H = 15 km. The simulations leading to Figures 7–10 are done with variable crustal thickness as indicated in the figure.

seismogenic upper crust governed by the damage rheology of LYAKHOVSKY *et al.* (1997).

2.5. Coupled Evolution of Earthquakes and Faults in a Regional Lithospheric Model

LYAKHOVSKY *et al.* (2001) and BEN-ZION *et al.* (1999) studied properties of crustal deformation associated with coupled evolution of earthquakes and faults using a version of the model shown in Figure 4 with a uniform upper crust thickness. The model consists of a seismogenic upper crust layer governed by the damage rheology of LYAKHOVSKY *et al.* (1997) over a layered Maxwell viscoelastic substrate. The evolving damage in the seismogenic layer simulates the creation and healing of fault systems as a function of the deformation history. The upper crust is coupled viscoelastically to the substrate where steady plate motion drives the deformation. The calculations employ vertically averaged variables of the thin sheet approximation for the viscous component of motion, and a Green function for a 3-D elastic half-space for the instantaneous component of deformation. Because of the thin sheet approximation, each model earthquake breaks the entire seismogenic zone so the smallest simulated event has a magnitude of about M = 6. In this sense the model is 2-D; however, stress transfer calculations are done, as mentioned above, with 3-D

elasticity. We refer to this combined framework as a 2.5-D hybrid model. The formulation accounts in an internally consistent manner for evolving deformation fields, evolving fault structures, and spatio-temporal seismicity patterns. Simplified simulations with a prescribed narrow damage zone in an otherwise damage-free plate generate earthquake cycles on a large strike-slip fault with distinct inter-, pre-, co-, and post-seismic periods. LYAKHOVSKY *et al.* (2001) established that model evolution during each period is controlled by a subset of parameters that can be constrained by seismological, geodetic, and other geophysical data. Parameter values that are compatible with observations associated with the San Andreas fault are indicated in Figure 4 and used in the simulations discussed below.

Model realizations with the large-scale parameters of Figure 4 and random initial damage distribution produce large crustal faults and subsidiary branches with complex geometries. The parameter-space studies of BEN-ZION *et al.* (1999) and LYAKHOVSKY *et al.* (2001) with random initial damage and uniform upper crust thickness indicate that the results may be divided into three different dynamic regimes controlled by the ratio of time scale for damage healing τ_H to time scale for tectonic loading τ_L. The former characterizes the time for strength recovering after the occurrence of a brittle event and the latter the time for stress recovering at a failed location. High ratio of τ_H/τ_L leads to the development of geometrically regular fault systems and FS event statistics compatible with the characteristic earthquake (CE) distribution. In such cases, the event statistics are similar to those simulated by planar model realizations of BEN-ZION and RICE (1993, 1995) and BEN-ZION (1996) with relatively regular quenched heterogeneities. Conversely, low ratio of τ_H/τ_L leads to the development of a network of disordered fault systems, and power-law Gutenberg-Richter (GR) distribution. In these cases, the event statistics are similar to those simulated by model realizations of Ben-Zion and Rice with highly disordered quenched heterogeneities. For intermediate ratios of τ_H/τ_L, the results exhibit alternating overall switching of response, from periods of intense seismic activity and CE statistics to periods of low seismic activity and GR statistics. DAHMEN *et al.* (1998) demonstrated analytically and numerically that a similar mode switching behavior exists in the planar model of Ben-Zion and Rice for a range of dynamic weakening and conservation of stress transfer parameters.

Figure 5 shows cumulative Benioff strain simulated by the regional lithospheric model with a uniform upper crust thickness $H = 15$ km for cases producing the CE distribution, mode switching activity, and GR statistics. In the top panel with the CE distribution, the deviations from linear cumulative Benioff strain before the large events are abrupt and cannot be approximated well with a power-law relation. In the middle panel, there is a sharp transition in the cumulative Benioff strain when the mode of seismic release switches around 32 yr. from a period with relatively low release and GR distribution to a period with relatively high release and CE distribution. In the bottom panel with seismicity having GR statistics, there is a clear phase of ASR before the largest event. The cumulative Benioff strain in the ASR

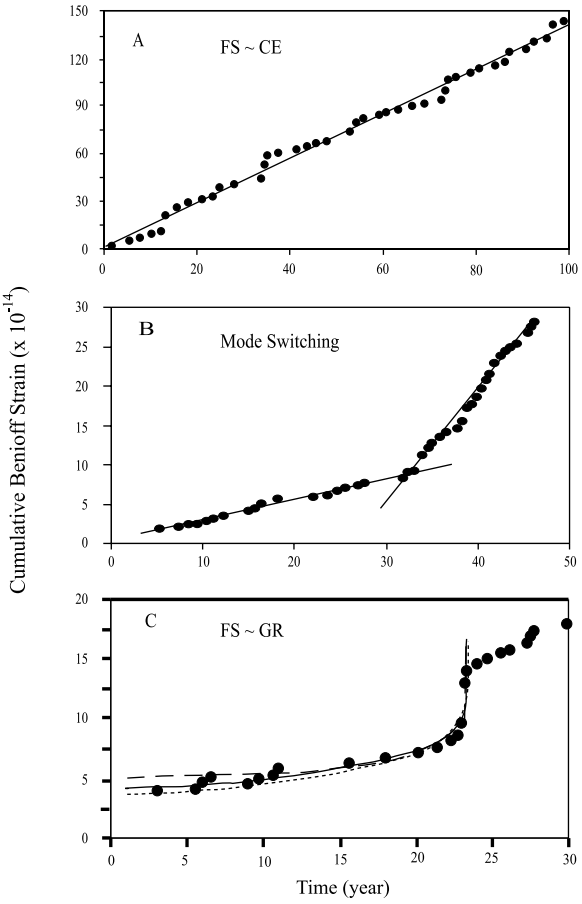

Figure 5
Cumulative Benioff strain for model realizations with uniform crustal thickness and three different ratios of healing time scale τ_H to loading time scale τ_L leading to different frequency-size (FS) distributions. (A) High ratio of τ_H/τ_L with characteristic earthquake distribution. (B) Intermediate ratio of τ_H/τ_L with mode switching activity. (C) Low ratio of τ_H/τ_L with power law FS statistics. The cumulative Benioff strain exhibits ASR before large events only when the earthquakes preceding the large event have a broad FS distribution. The ASR phase in the bottom panel is fitted with three power-law time-to-failure relations represented by $A_1 + A_2 t + A_3(t_f - t)^m$. The long dash line corresponds to eq. (13) and is given by $m = -1/3, A_1 = 1.4\ 10^{15}$, $A_2 = 0$, and $A_3 = 8\ 10^{13}$. The solid line corresponds to eq. (16) and is given by $m = 0.2, A_1 = 1.6\ 10^{15}$, $A_2 = 0$, and $A_3 = -1.0\ 10^{14}$. The short dash corresponds to eq. (17) and is given by $m = 1/3$, $A_1 = 1.6\ 10^{15}$, $A_2 = 1.2\ 10^{12}$, and $A_3 = -8.2\ 10^{13}$.

phase of the bottom panel can be fitted well by the singular power-law time-to-failure equation (13) with $m = -1/3$ (long dash curve), the nonsingular relation (16) with $m = 0.2$ (solid curve), and the generalized equation (17) with $m = 1/3$ (short dash curve). The good fits generated by the three different functions highlight the non-uniqueness associated with fitting such data, and stress the need for a careful

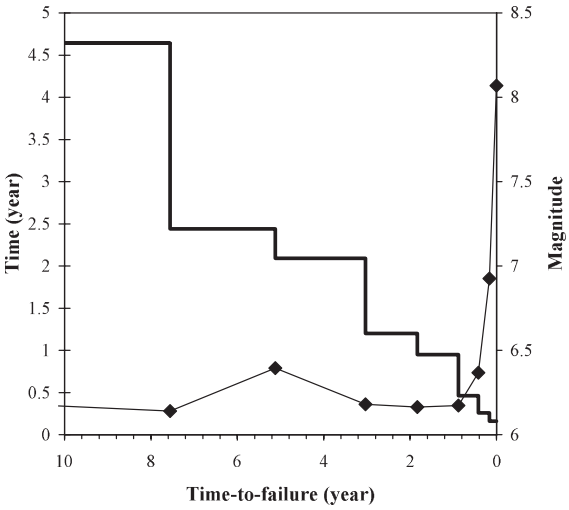

Figure 6
Average time interval between events (thick gray line) and average event magnitude (diamonds and thin line) during the ASR phase in the bottom panel of Figure 5.

estimation procedure when deriving functional forms and parameter values from similar data sets. VERE-JONES *et al.* (2001) provide several other examples of nonuniqueness and parameter estimation issues associated with ASR.

It is interesting to examine whether the activation process during the ASR phases involves increasing event size with time, increasing seismicity rates, or both. Figure 6 gives the average time interval between earthquakes and average event size in the ten years prior to the time t_f of the large event culminating the ASR phase in the bottom panel of Figure 5. The results show that the simulated ASR phase begins at about 8 years before t_f with increasing rates of moderate events (recall that the minimum simulated magnitude is $M \approx 6$), and the rates continue to accelerate as the time of the culminating large earthquake is approached. This initial form of activation is followed a few years later, at about 1 year before t_f in the example shown, by a shorter phase of increasing event sizes. Similar trends are found in another set of simulations discussed below.

To verify the conclusions associated with the previous simulations we modify the model to include a variable crustal thickness in the direction parallel to the plate motion. In this version (Fig. 4), the thickness of the brittle upper crust changes from 10 km to 20 km through a narrow smooth transition zone. The rheological parameters are the same as before and the ratio of τ_H/τ_L is low enough to produce GR event statistics in the previous configuration with a uniform crustal thickness. To account for the variable thickness of the upper crust, we include in the governing equations of the 2.5-D hybrid model an additional force term proportional to the gradient of the upper crust thickness, as is commonly done in studies of lithospheric

deformation (e.g., ARTUSHKOV, 1973; SONDER and ENGLAND, 1989). This amounts to replacing equation (13) of LYAKHOVSKY *et al.* (2001) with

$$H \iint\limits_{S} \mathrm{G}_{kn} \frac{\partial}{\partial t} \frac{\partial \sigma_{nm}}{\partial x_m} d\mathrm{S} + \frac{Hh}{\eta} \left(\frac{\partial \sigma_{km}}{\partial x_m} + \frac{\rho_{uc}(\rho_{lc} - \rho_{uc})}{2\rho_{lc}} g \nabla H^2 \right) = \frac{\partial u_k}{\partial t} - V_{plate}^{(k)} \ , \qquad (18)$$

where ρ_{uc} and ρ_{lc} are densities of the upper and lower crust layers, g is the gravitational acceleration, G is Green function for a 3-D elastic half space, u is displacement, and the other parameters are defined in Figure 4.

In our case with $\rho_{lc} - \rho_{uc} = 0.2$ gr/cm^3 and a mild difference between the thickness of the different crustal blocks, the additional force in (18) plays an insignificant role. However, the two different upper crust layers can store different amounts of elastic strain energy and produce different maximum earthquakes. This leads to another type of mode switching activity with space-time separation between event population with broad FS statistics and event population following the CE distribution (Fig. 7). During certain time intervals, seismicity not including the largest possible events occurs primarily in the thinner crustal block with FS statistics following the GR distribution. Occasionally, ruptures break through the transition zone initiating time intervals in which the thicker block participates in the earthquake activity. The seismicity in these time intervals includes clusters of the largest possible earthquakes and the associated FS statistics follows the CE distribution. During these latter periods, the cumulative Benioff strain experiences large abrupt jumps before the strongest events (Fig. 8) that cannot be fitted well by a power-law time-to-failure equation. In contrast, during the time intervals in which seismicity with broad FS statistics occurs in the thinner crustal block, the largest events are preceded by ASR phases (Fig. 9a) with a gradual buildup of activity. The cumulative Benioff strain in the ASR phases can be fitted well (Fig. 9b), as in Figure 5, by the singular analytical relation (13) with $m = -1/3$ (long dash curve), the non-singular equation (16) with $m = 0.2$ (solid curve), and the generalized relation (17) with $m = 1/3$ (short dash curve). Figure 10 displays the average time interval and average event size during the ASR phase of Figure 9b. As in Figure 6, the ASR phase begins with increasing rates of moderate events, here around 5 years before t_f, followed at about 3 years before t_f by increasing event sizes.

3. Discussion

We examined properties of ASR and related aspects of seismicity patterns associated with a number of theoretical frameworks. The studies continue our previous investigations of collective behavior of earthquakes and faults based on several different model categories. These include the discrete fault system with quenched heterogeneities of Section 2.3, the regional lithospheric model of Section

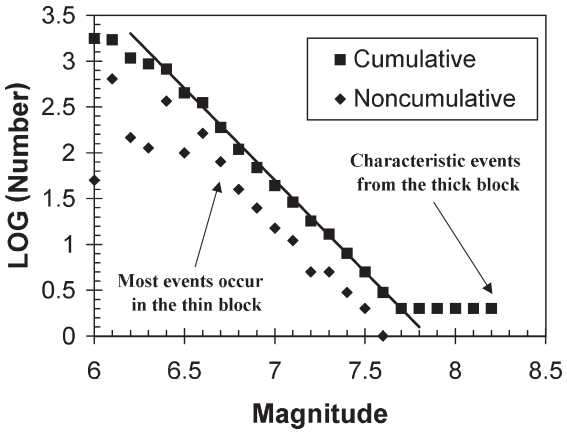

Figure 7
Frequency-size event statistics in model simulations with a variable upper crust thickness. Activity in the thinner block follows approximately a power-law distribution. Activity in the thicker block includes clusters of large events following the characteristic earthquake distribution.

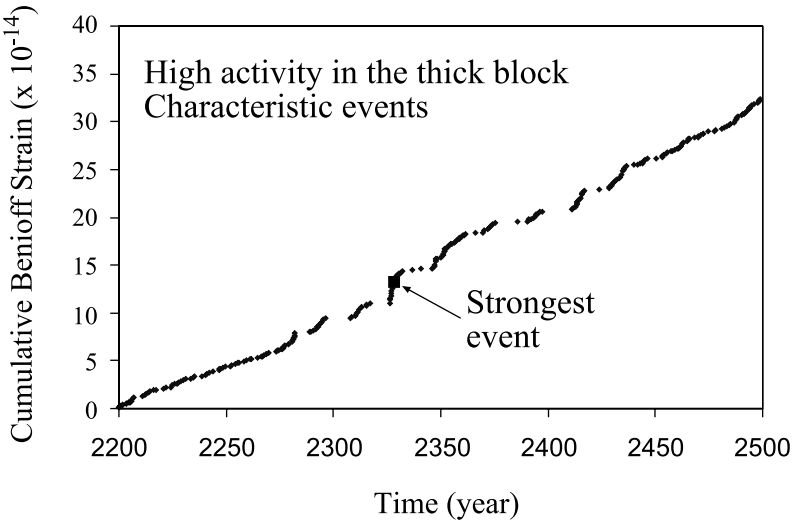

Figure 8
Cumulative Benioff strain release during a time interval with high activity in the thicker upper crust block. ASR phases are not observed.

2.5, and a smooth homogeneous fault in a continuum solid (e.g., BEN-ZION and RICE, 1997; LAPUSTA *et al.*, 2000). The results from all these models indicate the existence of three basic dynamic regimes. The first is associated with strong fault heterogeneities, power-law FS statistics of earthquakes, and random or clustered temporal statistics of intermediate and large events. The second is associated with

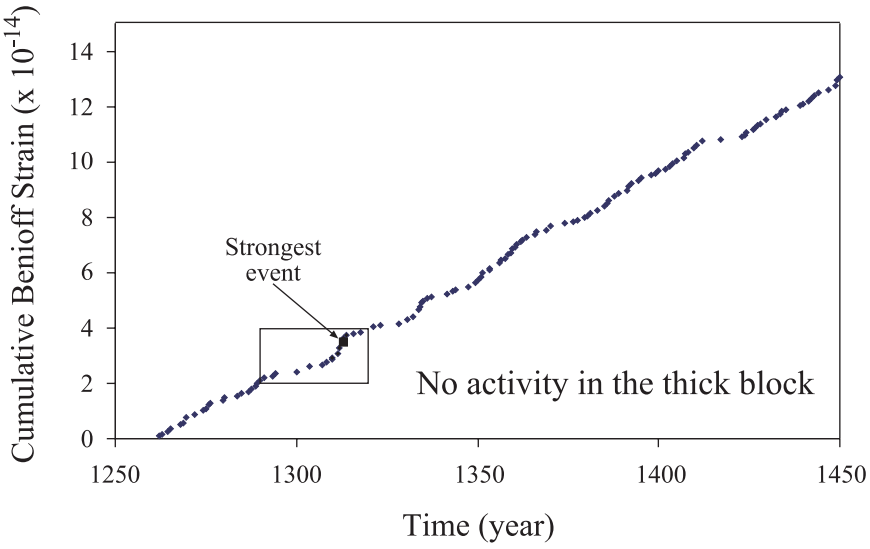

Figure 9a
Cumulative Benioff strain release for a time interval without activity in the thicker upper crust block. ASR phases are observed. The box marks an ASR phase that is fitted in Figure 9b.

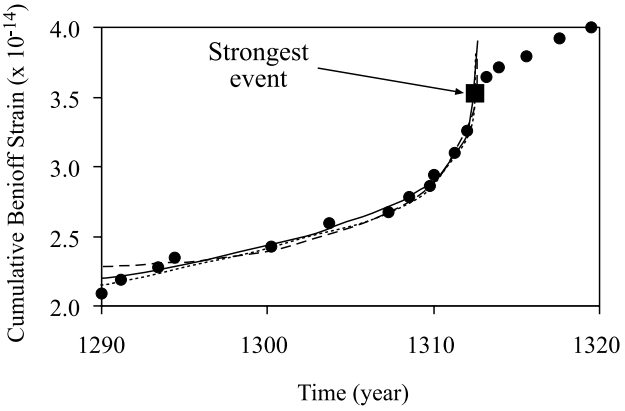

Figure 9b
Power-law time-to-failure fits to the ASR phase marked in Figure 9a with $A_1 + A_2 t + A_3(t_f - t)^m$. The long corresponds to eq. (13) and is given by $m = -1/3$, $A_1 = 1.8\ 10^{14}$, $A_2 = 0$, and $A_3 = 1.4\ 10^{14}$. The solid line corresponds to eq. (16) and is given by $m = 0.2$, $A_1 = 4.3\ 10^{14}$, $A_2 = 0$, and $A_3 = -1.1\ 10^{14}$. The short dash line corresponds to eq. (17) and is given by $m = 1/3$, $A_1 = 3.6\ 10^{14}$, $A_2 = -1.9\ 10^{11}$, and $A_3 = -4.7\ 10^{13}$.

homogeneous or relatively regular faults, FS statistics compatible with the characteristic earthquake distribution, and quasi-periodic temporal occurrence of large events. For a range of parameters, there is a third regime in which the response

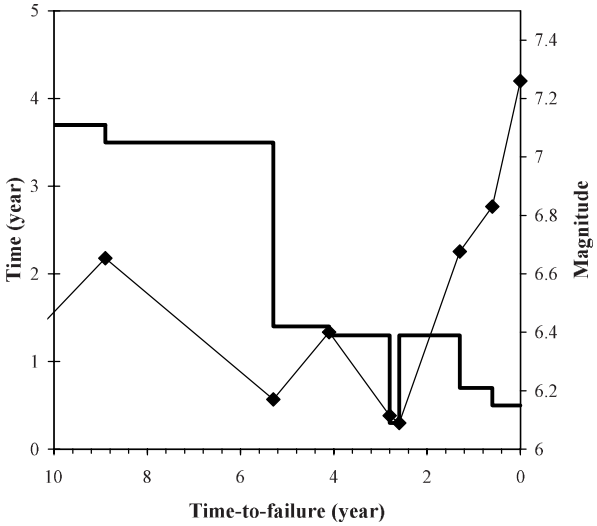

Figure 10
Average time interval between events (thick gray line) and average event magnitude (diamonds and thin line) in the ASR phase of Figure 9b

switches back and forth between the forgoing two modes of behavior. As discussed in our previous works, the model attributes and simulated patterns associated with the different dynamic regimes are compatible with friction, fracture, and other data of rock mechanics experiments, and *in situ* observations spanning wide ranges of space and time scales. The latter include fault trace maps and compiled earthquake statistics (WESNOUSKY, 1994; STIRLING *et al.*, 1996), high-resolution microseismicity patterns (e.g., JOHNSON and MCEVILLY, 1995; NADEAU *et al.*, 1995), and long paleoseismic records (e.g., GERSON *et al.*, 1993; MARCO *et al.*, 1996; ROCKWELL *et al.*, 2001; AMIT *et al.*, 2001).

In the present work we focus on connections between ASR and other properties of seismicity patterns. Various observational studies (e.g., BUFE and VARNES, 1993; BOWMAN *et al.*, 1998; BREHM and BRAILE, 1998; ROBINSON, 2000) fitted cumulative Benioff strain to power-law time-to-failure equation with exponent values m close to 0.3 (Table 1 and Fig. 1). Examining the subcritical crack growth process, we find that during the transition from stable slip to dynamic failure this framework predicts great variability and low asymptotic values of m that are not compatible with observations. Statistical physics results (e.g., SORNETTE and SAMMIS, 1995; SALEUR *et al.*, 1996; RUNDLE *et al.*, 2000b) provide scaling relations for deformation leading to global failures, assuming that those correspond to critical or spinodal phase transitions. Generic expectations in these models include progressive establishment of long-range correlations and asymptotic power-law relations during the final stages of the evolution.

One fundamental obstacle of progress toward a better understanding of earthquake processes is the fact that the evolution of stress and other governing dynamic variables on natural faults cannot be directly observed. We demonstrate that large earthquakes in the discrete heterogeneous fault model of BEN-ZION (1996) are associated with nonrepeating cyclical establishment and destruction of long-range stress correlations accompanied by non-stationary cumulative Benioff strain. These results are compatible with the idea that large earthquake cycles involve an approach to and retreat from criticality. Since stress evolution is not directly observable, it is important to find seismicity-based parameters that can be used as surrogate variables for stress and other dynamic variables of interest. This may be done by continuing studies of the type discussed in Section 2.3, combined with advanced analysis (e.g., PEPKE *et al.*, 1994; ENEVA and BEN-ZION, 1997; RUNDLE *et al.*, 2000a) of the associated seismicity parameters.

Damage mechanics provides a framework that can be used to model brittle deformation in a region with evolving material properties. We show analytically that a 1-D version of the damage rheology of LYAKHOVSKY *et al.* (1997) leads to a singular power-law time-to-failure relation with $m = -1/3$ for strain preceding catastrophic failure, and a corresponding nonsingular equation for cumulative Benioff strain release with $m = 1/3$. An approximate generalization of the latter result for regional deformation is obtained by adding a linear function of time representing a stationary background cumulative Benioff strain release.

Having these analytical expectations, we analyze results obtained by numerical simulations employing various realizations of a regional lithospheric model with a seismogenic upper crust governed by the damage rheology of LYAKHOVSKY *et al.* (1997). The simulations indicate that ASR phases exist only when the events before a given large earthquake have broad FS statistics. This appears to be a clear necessary condition; however it is not a sufficient one. That is because the existence of ASR requires not only a broad distribution of event sizes but also a failure sequencing within the distribution that produces increasing seismic release. The ASR phases in the simulated data are associated with both increasing rates of moderate events and increasing average event size; with the former starting a few years before the latter (Figs. 6 and 10). The simulated rate increase of moderate events is compatible with the observations of ELLSWORTH *et al.* (1981), LINDH (1990), SYKES and JAUMÉ (1990), and KNOPOFF *et al.* (1996), among others. The simulated increase of average earthquake size is compatible with the observations of JAUMÉ and SYKES (1999) and JAUMÉ (2000). The earlier occurrence in the simulations of the former type of activation and generality of the other results should be examined further in future studies.

The cumulative Benioff strain in the simulated ASR phases can be fitted well by the singular, nonsingular, and generalized nonsingular functions discussed above with exponent values close to those of the analytical derivations and observational results. The good fit obtained with all three functions emphasizes the non-uniqueness

associated with fitting such data sets and the need for better estimation procedures (see also VERE-JONES *et al.*, 2001). It is also important to develop better procedures for selecting space-time domains associated with ASR phases, and to examine whether the "zonings" of previous observational works (e.g., BOWMAN *et al.*, 1998; BREHM and BRAILE, 1998; ROBINSON, 2000; ZOLLER *et al.*, 2001) remain valid for future ASR phases.

The results of this and other works point to the existence of two complementary endmember predictive signals in patterns of moderate and large events associated with the first two dynamic regimes summarized at the beginning of the discussion. On regular fault systems with FS event statistics compatible with the CE distribution, there is predictive information in the associated quasi-periodic temporal distribution of large events. On highly disordered fault systems with power-law FS statistics and random or clustered temporal distribution of large events, phases of ASR before large events have predictive information. Mode switching behavior, mixed populations of faults, and various forms of transients are some examples among many possible complicating factors. A continuing multi-disciplinary research employing a combination of numerical simulations, analytical work, and advanced analysis of synthetic and observed data can clarify the generality of the discussed results and may lead to recognition of additional predictive signals. Further progress in prediction studies will also require more rigorous hypothesis testing and data analysis (e.g., KAGAN, 1999).

Acknowledgments

The results of Figure 3 are taken from work in progress of YBZ with Mariana Eneva and Yunfeng Liu. Yueqiang Huang helped to prepare Figure 1. We thank anonymous reviewers for comments. YBZ acknowledges support from the National Science Foundation (grant EAR-9725358) and the Southern California Earthquake Center (based on NSF cooperative agreement EAR-8920136 and USGS cooperative agreement 14-08-0001-A0899). VL acknowledges support from the United States – Israel Binational Science Foundation (BSF), Jerusalem Israel (grant No. 9800198).

REFERENCES

AMIT, R., ZILBERMAN, E., PORAT, N., and ENZEL, Y. (2002), *Paleoseismic Evidence for Time-dependency of Seismic Response on a Fault System – The Southern Arava Valley, Red Sea Rift, Israel*, Geol. Soc. Am. Bull. *114*, 192–206.

ARTUSHKOV, E. V. (1973), *Stresses in the Lithosphere Caused by Crustal Thickness Inhomogeneities*, J. Geophys. Res. *78*, 7675–7708.

ATKINSON, B. K. and MEREDITH, P. G. *The theory of subcritical crack growth with applications to minerals and rocks*. In: *Fracture Mechanics of Rock* (B. K. Atkinson, ed.), (Academic Press, San Diego 1987), pp. 110–166.

BEN-ZION, Y. (1996), *Stress, Slip and Earthquakes in Models of Complex Single-fault Systems Incorporating Brittle and Creep Deformations*, J. Geophys. Res. *101*, 5677–5706.

BEN-ZION, Y., DAHMEN, K., LYAKHOVSKY, V., ERTAS, D., and AGNON, A. (1999), *Self-driven Mode Switching of Earthquake Activity on a Fault System*, Earth Planet. Sci. Lett. *172*/1–2, 11–21.

BEN-ZION, Y. and RICE, J. R. (1993), *Earthquake Failure Sequences along a Cellular Fault Zone in a Three-dimensional Elastic Solid Containing Asperity and Nonasperity Regions*, J. Geophys. Res. *98*, 14,109–14,131.

BEN-ZION, Y. and RICE, J. R. (1995), *Slip Patterns and Earthquake Populations along Different Classes of Faults in Elastic Solids*, J. Geophys. Res. *100*, 12,959–12,983.

BEN-ZION, Y. and RICE, J. R. (1997), *Dynamic Simulations of Slip on a Smooth Fault in an Elastic Solid*, J. Geophys. Res. *102*, 17,771–17,784.

BEN-ZION, Y. and SAMMIS, C. G. (2001), *Characterization of Fault Zones*, Pure Appl. Geophys., in press.

BOWMAN, D. D., OUILLON, G., SAMMIS, C. G., SORNETTE, A., and SORNETTE, D. (1998), *An Observational Test of the Critical Earthquake Concept*, J. Geophys. Res. *103*, 24,359–24,372.

BREHM, D. J. and BRAILE, L. W. (1998), *Intermediate-term Earthquake Prediction Using Precursory Events in the New Madrid Seismic Zone*, Bull. Seismol. Soc. Am. *88*, 564–580.

BUFE, C. G. and VARNES, D. J. (1993), *Predictive Modeling of the Seismic Cycle of the Greater San Francisco Bay Region*, J. Geophys. Res. *98*, 9871–9883.

BUFE, C. G., NISHENKO, S. P., and VARNES, D. J. (1994), *Seismicity Trends and Potential for Large Earthquakes in the Alaska-Aleutian Region*, Pure Appl. Geophys. *142*, 83–99.

CHARLES, R. J. (1958), *Static Fatigue of Glass*, J. Appl. Physics *29*, 1549–1560.

COX, S. J. D. and SCHOLZ, C. H. (1988), *Rupture Initiation in Shear Fracture of Rocks: An Experimental Study*, J. Geophys. Res. *93*, 3307–3320.

DAHMEN, K., ERTAS, D., and BEN-ZION, Y. (1998), *Gutenberg Richter and Characteristic Earthquake Behavior in Simple Mean-field Models of Heterogeneous Faults*, Phys. Rev. E *58*, 1494–1501.

DAS, S. and SCHOLZ, C. H. (1981), *Theory of Time-dependent Rupture in the Earth*, J. Geophys. Res. *86*, 6039–6051.

DIETERICH, J. H. (1972), *Time-dependent Friction in Rocks*. J. Geophys. Res. *77*, 3690–3697.

ELLSWORTH, W. L., LINDH, A. G., PRESCOTT, W. H., and HERD, D. J. *The 1906 San Francisco Earthquake and the seismic cycle*. In *Earthquake Prediction: An Internation Review*, Maurice Ewing Ser., vol. 44, (eds. D.W. Simpson and P.G. Richards), (AGU, Washington, D.C. 1981) pp. 126–140.

ENEVA, M. and BEN-ZION, Y. (1997), *Application of Pattern Recognition Techniques to Earthquake Catalogs Generated by Models of Segmented Fault Systems in Three-dimensional Elastic Solids*, J. Geophys. Res. *102*, 24,513–24,528.

ENEVA, M. and BEN-ZION, Y. (1999), *Criticality in Stress/Slip Distribution and Seismicity Patterns in Fault Models*, EOS Trans. Amer. Geophys. Union *80*, S331.

FERGUSON, C. D. (1997), *Numerical Investigations of an Earthquake Fault Based on a Cellular Automaton, Slider-block Model*, Ph.D. Dissertation, Boston University.

FISHER, D. S., DAHMEN, K., RAMANATHAN, S., and BEN-ZION, Y. (1997), *Statistics of Earthquakes in Simple Models of Heterogeneous Faults*, Phys. Rev. Lett. *78*, 4885–4888.

GERSON, R., GROSSMAN, S., AMIT, R., and GREENBAUM, N. (1993), *Indicators of Faulting Events and Periods of Quiescence in Desert Alluvial Fans*, Earth Surface Processes and Landforms *18*, 181–202.

HUANG, Y., SALEUR, H., JOHANSEN, A., LEE, M., and SORNETTE, D. (2000), *Artifactual Log-periodicity in Finite Size Data: Relevance for Earthquake Aftershocks*, J. Geophys. Res. *105*, 25,451–25,471.

INGRAFFEA, A. R. *Theory of crack initiation and propagation in rock*. In *Fracture Mechanics of Rock* (B. K. Atkinson, ed.) (Academic Press, San Diego 1987) pp. 76–110.

JAUMÉ, S. C. (2000), *Changes in earthquake size-frequency distributions underlying accelerating seismic moment/energy release*. In Geophys. Mono. Series 120, *GeoComplexity and the Physics of Earthquakes* (J. B. Rundle, D. L. Turcotte, and W. Klein, eds.) 199–210 (American Geophysical Union, Washington D. C).

JAUMÉ, S. C. and SYKES, L. R. (1999), *Evolving Toward a Critical Point: A Review of Accelerating Seismic Moment/Energy Release Prior to Large and Great Earthquakes*, Pure Appl. Geophys. *155*, 279–305.

JENSEN, H. J. *Self-organized Criticality* (Cambridge University Press 1998).

JOHNSON, P. and MCEVILLY, T. V. (1995), *Parkfield Seismicity: Fluid-driven*? J. Geophys. Res. *100*, 12,937–12,950.

JONES, L. M. and MOLNAR, P. (1979), *Some Characteristics of Foreshocks and their Possible Relationship to Earthquake Prediction and Premonitory Slip on Faults*, J. Geophys. Res. *84*, 3596–3608.

KAGAN, Y. Y. (1999), *Is Earthquake Seismology a Hard, Quantitative Science*?, Pure Appl. Geophys. *155*, 233–258.

KANAMORI, H. and ANDERSON, D. L. (1975), *Theoretical Basis of Some Empirical Relations in Seismology*, Bull. Seismol. Soc. Am. *65*, 1073–1095.

KEILIS-BOROK, V. I. and KOSSOBOKOV, V. G. (1990), *Premonitory Activation of Earthquake Flow: Algorithm M8*, Phys. Earth Planet. Inter. *61*, 73–83.

KNOPOFF, L., LEVSHINA, T., KEILIS-BOROK, V. I., and MATTONI, C. (1996), *Increased long-range Intermediate-magnitude Earthquake Activity prior to Strong Earthquakes in California*, J. Geophys. Res. *101*, 5779–5796.

LAPUSTA, N., RICE, J. R., BEN-ZION, Y., and ZHENG, G. (2000), *Elastodynamic Analysis for Slow Tectonic Loading with Spontaneous Rupture Episodes on Faults with Rate- and State-dependent Friction*, J. Geophys. Res. *105*, 23,765–23,789.

LINDH, A. G. (1990), *The Seismic Cycle Pursued*, Nature *348*, 580–581.

LYAKHOVSKY, V. (2001), *Scaling of Fracture Length and Distributed Damage*, Geophys. J. Int. *144*, 114–122.

LYAKHOVSKY, V., BEN-ZION, Y., and AGNON, A. (1997), *Distributed Damage, Faulting, and Friction*, J. Geophys. Res. *102*, 27,635–27,649.

LYAKHOVSKY, V., BEN-ZION, Y., and AGNON, A. (2001), *Earthquake Cycle, Fault Zones, and Seismicity Patterns in a Rheologically Layered Lithosphere*, J. Geophys. Res. *106*, 4103–4120.

MAIN, I. G. (1999), *Applicability of Time-to-failure Analysis to Accelerated Strain before Earthquakes and Volcanic Eruptions*, Geophys. J. Int. *139*, F1–F6.

MARCO, S., STEIN, M., AGNON, A., and RON, H. (1996), *Long-term Earthquake Clustering: A 50,000 Year Paleoseismic Record in the Dead Sea Graben*, J. Geophys. Res. *101*, 6179–6192.

MARONE, C. (1998), *Laboratory-derived Friction Laws and their Application to Seismic Faulting*, Annu. Rev. Earth Planet. Sci. *26*, 643–649.

MEREDITH, P. G. and ATKINSON, B. K. (1985), *Fracture Toughness and Subcritical Crack Growth during High-temperature Tensile Deformation of Westerly Granite and Black Gabbro*, Tectonophysics *39*, 33–51.

MOGI, K. (1969), *Some Features of Recent Seismic Activity in and near Japan* {2}*: Activity Before and After Great Earthquakes*, Bull. Eq. Res. Inst. Univ. Tokyo *47*, 395–417.

MOGI, K. *Seismicity in Japan and long-term earthquake forecasting*. In *Earthquake Prediction: An Internation Review*, Maurice Ewing Ser., vol. 4 (eds. D.W. Simpson and P.G. Richards) pp. 43–51, (AGU, Washington, D.C. 1981).

NADEAU, R. M., FOXALL, W., and MCEVILLY, T. V. (1995), *Clustering and Periodic Recurrence of Microearthquakes on the San Andreas Fault at Parkfield, California, Science 267*, 503–507.

PAPAZACHOS, B. C. (1973), *The Time Distribution and Prediction of Reservoir-associated Foreshock and its Importance to the Prediction of the Principal Shock*, Bull. Seismol. Soc. Am. *63*, 1973–1978.

PARIS, P. C. and ERDOGAN, F. (1963), *A Critical Analysis of Crack Propagation Laws*, J. Basic Engineering, ASME Transactions, Series D *85*, 528–534.

PEPKE, S. L., CARLSON, J. M., and SHAW, B. E. (1994), *Prediction of Large Events on a Dynamical Model of a Fault*, J. Geophys. Res. *99*, 6769–6788.

PRESS, F. and ALLEN, C. (1995), *Patterns of Seismic Release in the Southern California Region*, J. Geophys. Res. *100*, 6421–6430.

ROBINSON, R. (2000), *A Test of the Precursory Accelerating Moment Release Model on Some Recent New Zealand Earthquakes*, Geophys. J. Int. *140*, 568–576.

ROCKWELL, T. K., LINDVALL, S., HERZBERG, M., MURBACH, D., DAWSON, T., and BERGER, G. (2000), *Paleoseismology of the Johnson Valley, Kickcapoo and Homestead Valley Faults of the Eastern California Shear Zone*, Bull. Seismol. Soc. Am. *90*, 1200–1236.

RUNDLE, J. B., KLEIN, W., TIAMPO, K., and GROSS, S. (2000a), *Linear Patterns Dynamics in Nonlinear Threshold System*, Phys. Rev. E *61*, 2418–2431.

RUNDLE, J. B., KLEIN, W., TURCOTTE, D. L., and MALAMUD, B. D. (2000b), *Precursory Seismic Activation and Critical-point Phenomena*, Pure Appl. Geophys. *157*, 2165–2182.

SALEUR, H., SAMMIS, C. G., and SORNETTE, D. (1996), *Discrete Scale Invariance, Complex Fractal Dimensions, and Log-periodic Fluctuations in Seismicity*, J. Geophys. Res. *101*, 17,661–17,677.

SAMMIS, C. G. and SMITH, S. W. (1999), *Seismic Cycles and the Evolution of Stress Correlation in Cellular Automaton Models of Finite Fault Networks*, Pure Appl. Geophys. *155*, 307–334.

SAMMIS, C. G., SORNETTE, D., and SALEUR, H. *Complexity and earthquake forecasting*. In *Reduction and Predictability of Natural Disasters*, SFI Studies in the Sciences of Complexity, vol. XXV, (eds. J. B. Rundle, W. Klein, and D. L. Turcotte) pp. 143-156 (Addison-Wesley, Reading, Mass. 1996).

SCHOLZ, C. H. *The Mechanics of Earthquakes and Faulting* (Cambridge Press 1990).

SHAW, B. E., CARLSON, J. M., and LANGER, J. S. (1992), *Patterns of Seismic Activity Preceding Large Earthquakes*, J. Geophys. Res. *97*, 479–488.

SILVERMAN, B. W. *Density estimation for statistics and data analysis*. In *Monographs on Statistics and Applied Probability* (eds. D. R. Cox, D. V. Hinkley, D. Rubin and B. W. Silverman), 26 (Chapman and Hall, New York 1986).

SONDER, L. J. and ENGLAND, P. C. (1989), *Effects of a temperature-dependent Rheology on Large-scale Continental Extension*, J. Geophys. Res. *94*, 7603–7619.

SORNETTE, D. (1992), *Mean-field Solution of a Block-spring Model of Earthquakes*, J. Phys. I France *2*, 2089–2096.

SORNETTE, D. and SAMMIS, C. G. (1995), *Complex Critical Exponent from Renormalization Group Theory of Earthquakes: Implications for Earthquake Predictions*, J. Phys. I France, 5, 607–619.

STIRLING, M. W., WESNOUSKY, S. G., and SHIMAZAKI, K. (1996), *Fault Trace Complexity, Cumulative Slip, and the Shape of the Magnitude-frequency Distribution for Strike-slip Faults: A Global Survey*, Geophys. J. Int. *124*, 833–868.

SWANSON, P. L. (1984), Subcritical Crack Growth and Other Time and Environment-dependent Behavior in Crustal Rocks, J. Geophys. Res. *89*, 4137–4152.

SWANSON, P. L. (1987), *Tensile Fracture Resistance Mechanisms in Brittle Polycrystals: An Ultrasonics and in situ Microscopy Investigation*, J. Geophys. Res. *92*, 8015–8036.

SYKES, L. R. and JAUMÉ, S. C. (1990), *Seismic Activity on Neighboring Faults as a Long-term Precursor to Large Earthquakes in the San Francisco Bay Region*, Nature *348*, 595–599.

VARNES, D. J. (1989), *Predicting Earthquake by Analyzing Accelerating Precursory Seismic Activity*, Pure Appl. Geophys. *130*, 661–686.

VARNES, D. J. and BUFE, C. G. (1996), *The Cyclic and Fractal Seismic Series Preceding an* $M_b = 4.8$ *Earthquake on 1980 February 14 near the Virgin Islands*, Geophys. J. Int. *124*, 149–158.

VERE-JONES, D., ROBINSON, R., and YANG, W. (2001), *Remarks on the Accelerated Moment Release Model: Problems of Model Formulation, Simulation and Estimation*, Geophys. J. Int. *144*, 517–531.

WESNOUSKY, S. G. (1994), *The Gutenberg-Richter or Characteristic Earthquake Distribution, which is it*?, Bull. Seismol. Soc. Am. *84*, 1940–1959.

ZOLLER, G., HAINZL, S., and KURTHS, J. (2001), *Observation of Growing Correlation Length as an Indicator for Critical Point Behavior prior to Large Earthquakes*, J. Geophys. Res. *106*, 2167–2175.

(Received February 20, 2001, revised June 11, 2001, accepted June 15, 2001)